International Journal of Nanomedicine

Dovepress
Taylor & Francis Group

Open Access Full Text Article

ORIGINAL RESEARCH

Polyethylenimine-Conjugated Au-NPs as an Efficient Vehicle for in vitro and in vivo DNA Vaccine Delivery

Aras Kartouzian[1], Alexandra Heiz[1], Kamyar Shameli[2,*], Hassan Moeini[3,*]

[1]Catalysis Research Center, School of Natural Sciences, Technical University of Munich, Munich, Germany; [2]Institute of Virology, School of Medicine, Technical University of Munich, Munich, Germany; [3]Iguana Biotechnology GmbH, Munich, Germany

*These authors contributed equally to this work

Correspondence: Kamyar Shameli; Hassan Moeini, Email kamyarshameli@gmail.com; moeini82@yahoo.com

Purpose: This study aimed to develop green-synthesized gold nanoparticles (Au-NPs) conjugated with polyethyleneimine (PEI) to overcome challenges in intracellular DNA vaccine delivery, focusing on enhancing cellular uptake and immune responses against the human norovirus (HuNoV) GII.4 variants.

Methods: Au-NPs were synthesized using a citrate-ion-mediated green approach, with size and morphology analyzed via UV-vis spectroscopy and transmission electron microscopy (TEM). Stability was evaluated through zeta potential measurements. PEI conjugation was employed to modify surface charge. After in vitro evaluation of pDNA delivery efficiency and cytotoxicity in HEK293 cells, PEI-coated Au-NPs loaded with a HuNoV GII.4 pDNA vaccine (AuPEI-NPs-pDNA) were assessed for the immune responses in mice.

Results: UV-vis spectroscopy and TEM confirmed successful Au-NP synthesis. Zeta potential shifted from −31.38 mV to −20.60 mV, reflecting stable but slightly reduced colloidal stability with larger sizes. PEI conjugation reversed surface charge to positive, enabling 100% transfection efficacy in HEK293 cells by day two without cytotoxicity. The AuPEI-NPs-pDNA induced significantly higher NoV-specific IgG antibodies and T-cell responses compared to unmodified Au-NPs, highlighting the role of positive charge in enhancing cellular uptake and immune activation. These results underscore PEI-coated Au-NPs as a biocompatible, efficient platform for DNA vaccine delivery.

Conclusion: PEI-coated Au-NPs demonstrate exceptional potential as non-toxic, high-efficiency carriers for DNA vaccines, enabling robust humoral and cellular immune responses. This strategy holds promises for advancing gene therapy and combating rapidly evolving pathogens like HuNoV, with broader applications in targeted drug delivery.

Keywords: gold nanoparticle, polyethylenimine, DNA vaccine, gene delivery, in vitro, in vivo

Introduction

Advancements in vaccine technology were increasingly focusing on DNA and RNA delivery vaccines, propelled by exploring nano vehicle materials like Au-NPs (Au-NPs) to augment their efficacy.[1] These microscopic structures offered a versatile platform for optimizing vaccine delivery owing to their unique characteristics.[2] Au-NPs, with their controllable size, customizable surface chemistry, and high surface area-to-volume ratio, were presenting an attractive option for improving DNA and RNA vaccine delivery.[3,4] Their size allowed for precise manipulation, ensuring efficient cellular uptake and biodistribution. Additionally, their surface chemistry could be tailored to enhance stability, target specific cell types, or modulate release kinetics, offering unprecedented control over vaccine delivery dynamics.[5]

By encapsulating or adsorbing nucleic acids onto their surfaces, Au-NPs can shield the vaccine payload from enzymatic degradation and immune recognition, thereby prolonging its circulation time in the body and enhancing its bioavailability.[6] Furthermore, the inherent biocompatibility of Au-NPs ensured minimal cytotoxicity and immunogenicity, making them safe

Received: 1 January 2025
Accepted: 22 March 2025
Published: 1 April 2025

carriers for in vivo applications.[7] Their ability to navigate biological barriers and penetrate cellular membranes facilitated the efficient delivery of DNA vaccines to target cells or tissues, thereby eliciting robust immune responses. These features have positioned Au-NPs as promising delivery vehicles for DNA-based vaccines.[8]

The green synthesis of Au-NPs via the Turkevich method offered a sustainable and environmentally friendly approach to nanoparticle production.[9] The use of biocompatible and non-toxic reagents made this synthesis method highly desirable for various biomedical applications. Additionally, the Turkevich method produced Au-NPs with well-defined sizes and shapes, which was crucial for ensuring uniformity and reproducibility in downstream applications.[10] Furthermore, the surface chemistry of Au-NPs synthesized could be easily modified to facilitate stable interactions with nucleic acids. This capability made the Turkevich method ideal for creating surface bonds with nucleic acids, offering a versatile platform for applications such as gene delivery, biosensing, and therapeutics.[11,12]

Polyethyleneimine (PEI) as a net-like polymeric network agent played a fundamental role in protecting nucleic acids linked with Au-NPs.[13] By creating a positive charge surface, this polymer was forming a stable and favorable electrostatic environment around negatively charged nucleic acids and protecting them from enzymatic degradation and immune detection.[14] This protective layer not only increases the stability and biocompatibility of the nucleic acid-Au-NPs complex but also facilitates efficient cellular uptake and intracellular delivery. Furthermore, the cationic nature of PEI promotes interactions with the negatively charged cell membrane, facilitating cellular internalization and endosomal escape, and ultimately leading to increased transfection efficiency.[15,16]

The research objectives of this study encompassed several key areas aimed at advancing the field of nucleic acid delivery vaccines using Au-NPs and PEI. Firstly, the study sought to investigate the efficacy of Au-NPs as carriers for DNA-based vaccines, focusing on their ability to enhance their bioavailability. This involved evaluating the stability, biocompatibility, and cellular uptake of Au-NP-nucleic acid complexes in vitro and in vivo. Secondly, the study aimed to optimize the synthesis of Au-NPs using the environmentally friendly Turkevich method, focusing on controlling size, shape, and surface chemistry to facilitate stable interactions with nucleic acids. This involved characterizing the physicochemical properties of Au-NPs and assessing their ability to form surface bonds with nucleic acids. Lastly, the research sought to elucidate the role of PEI as a protective and enhancing agent for nucleic acid delivery using Au-NPs.

Materials and Methods

Materials

Synthesis Chloroauric acid trihydrate ($HAuCl_4 \cdot 3H_2O$: ≥99.9% trace metals basis), Sodium citrate trihydrate (≥99.0%), sodium carbonate (≥99.5%), sodium hydrogen carbonate (≥99.7%), and bovine serum albumin (BSA) (≥98%) were purchased from Sigma-Aldrich (St. Louis, MO, USA) and polyethyleneimine HCl, Linear Mw 4000 (L-PEI HCl 4000) was purchased from Polysciences, Inc. (400 valleys, Warrington, PA 18976). All glassware used in the syntheses was thoroughly cleaned in aqua regia (HCl: HNO_3 = 3:1 v/v), rinsed in ultrapure water (18.2 MΩ·cm), and oven-dried before use.

Cells and DNA Plasmids

HEK293 cells (ATCC: CRL-1573™) were used for DNA transfection using DNA-loaded Au-NPs. The cells were maintained in RPMI 1640 Medium supplemented with 10% fetal bovine serum (FBS) (Gibco, USA). Cells were regularly tested for mycoplasma contamination to ensure reliability. DNA plasmid pMN-GII.4 encoding green fluorescence protein (GFP) and human norovirus GII.4 capsid (VP1) proteins (Figure 1) was propagated in *Escherichia coli* DH5α and purified using a Qiagen EndoFree Plasmid Maxi Kit (Qiagen, Germany). Plasmid purity and concentration were assessed using a NanoDrop spectrophotometer (Thermo Fisher Scientific, USA), ensuring an A260/A280 ratio *of 1.8–2.0*.

Preparation of Au-NPs (Au-NPs)

Briefly, 100 mL of 2.5 mm sodium citrate was heated to boiling in a 250 mL three-neck round-bottomed flask in a glycerol bath. When the solution begins to boil, 1 mL of 20 mm $HAuCl_4$ was added under vigorous stirring. After 10 minutes, the color of the solution turned soft pink, indicating the formation of Au-NP seeds.[17] For the growing steps,

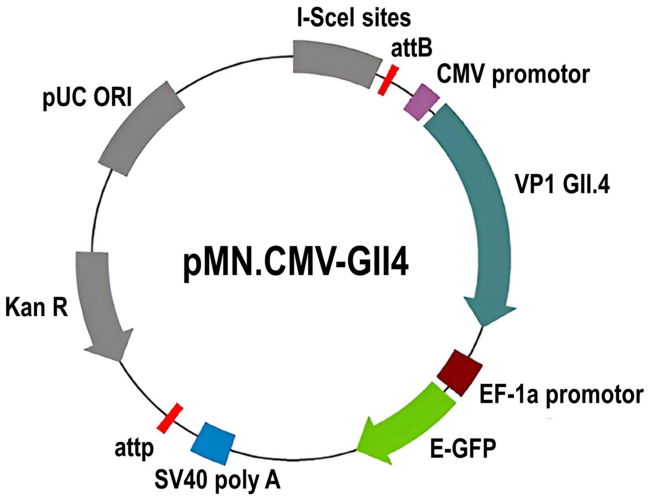

Figure 1 Map of the recombinant plasmid pMN-NoVGII4. The plasmid harbors the gene encodes norovirus GII.4 capsid proteins, regulated by the CMV promoter, and the green fluorescence protein (GFP), regulated by the EF-1α promoter.

the temperature of the solution was reduced to 90 °C, and 1 mL of 30 mm sodium citrate and 1 mL of 20 mm $HAuCl_4$ were successively added. This process was repeated every 30 min for a total of three times, resulting in a new generation of nanoparticles. After each interval, the sample was characterized to obtain information on the growth and size of the nanoparticles. Once the first-generation reaction was completed, the sample was diluted by extracting 55 mL of the sample and adding 53 mL of ultrapure water along with 1 mL of 30 mm sodium citrate.[18,19] This defines the seeds of the next generation of the Au-NPs, with which the same procedure being repeated for subsequent generations. The first generation showed a bright red color, indicating the onset of NP nucleation, while the second to fourth generations exhibited a stable red color that gradually darkened.

Preparation of PEI-Coated Au-NPs

The 4th generation of Au-NP was used to prepare its complex with cationic PEI by stirring Au-NPs in a 1 mg/mL solution of PEI (in 1 mm NaCl) for 30 minutes at room temperature (RT). The coated particles were purified by two steps of washing with 1 mm NaCl and centrifugation at 13000 *rpm* for 10 min. The AuPEI-NPs were kept in 1 mm NaCl for further characterization, as well as for in vitro and in vivo gene delivery assessment (Scheme 1).[20]

Characteristics of Au-NPs and Gold Hybrid Polymer Nanoparticles

UV-visible spectra for all generated Au-NPs were obtained using an Agilent Cary 60 UV-visible spectrophotometer (Agilent, Santa Clara, USA) measuring 300–800 nm. The hydrodynamic size and zeta-potential (ZP) of the Au-NPs were evaluated at 25°C using a Malvern Zetasizer Nano ZS-90 (Malvern, UK). Transmission electron microscopy (TEM, JEM-1200EX, JEOL Ltd., Tokyo, Japan) was used to determine the size and morphology of Au-NPs. Au-NPs were prepared by dropping a small amount of aqueous dispersion on copper grids, which were dried and then examined in the TEM. The size of Au-NPs was initially measured using the ImageJ (Fiji) software. Subsequently, the final size and distribution were statistically determined using SPSS-16 software.

Loading DNA Plasmids on Au-NPs

DNA-loaded nanoparticles were prepared by mixing 4 µg of the DNA plasmid pMN-NoVGII4 with 400 µL of Au- or AuPEI-NPs in 1 mm NaCl solution, followed by a 30-minute incubation at RT with shaking at 900 rpm. Subsequently, the DNA-loaded nanoparticles were precipitated at 6000 rpm for 10 minutes at RT and then washed with 1 mL of 1 mm NaCl solution to remove unbound DNA. Finally, the particles were resuspended in 400 µL of 1 mm NaCl solution for cell transfection.

https://doi.org/10.2147/IJN.S493211

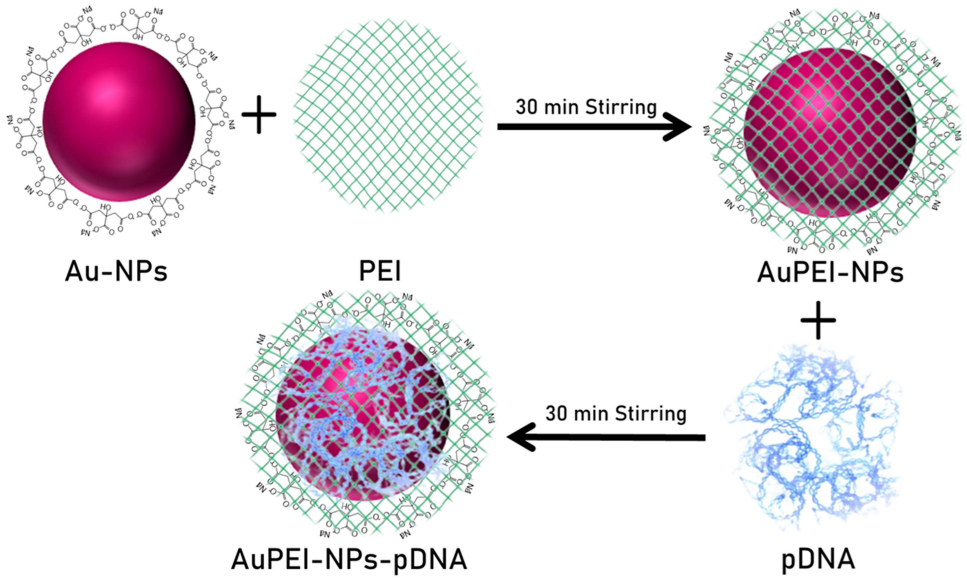

Scheme 1 An overview of the workflow used to crosslink polyethyleneimine (PEI) and plasmid DNA (pDNA) and then form a complex with Au-NPs (AuPEI-NPs-pDNA).

Plasmid Transfection of HEK293 Cells

The capability of the Au-NPs for in vitro gene delivery was assessed in HEK293 cells. To this end, HEK293 cells at 85% confluency in RPMI medium supplemented with 10% (v/v) FBS were treated with 400 µL DNA-loaded Au- or AuPEI-NPs at 37°C in a CO_2 incubator for 48 hours. The cells were monitored for green fluorescence protein expression, serving as an indicator of successful DNA delivery into the cells, over a two-day period.

Mice Immunization

Eight-week-old Female BALB/c mice (four per group) were intramuscularly injected with 100 µg of DNA plasmid pMN-GII.4VP1, or DNA-loaded Au-NPs or PEI-coated Au-NPs. PBS-injected mice served as negative controls. Mice were inoculated three times at two-week intervals. Mice were sacrificed, two weeks after the last administration, and NoV-specific immune responses were assessed in the immunized mice by ELISA and T-cell assay.

Antibody Titration by ELISA

Norovirus-specific serum IgG was measured in mice sera by a quantitative ELISA on 96-well plates coated with 2µg/mL NoV capsid protein.[20] To this end, after blocking with 5% milk powder in PBST (1×PBS containing 0.05% Tween 20) for two hours, the wells were treated with 1:1000 diluted mice sera in 1×PBS. After 2 h incubation at RT and subsequent washing steps (5×) with PBST, the wells were treated with HRP-conjugated anti-mouse secondary antibody for 1 hour at RT. Following another round of washing (5×), bound antibodies were detected by adding 100µL of TMB substrate solution at RT in the dark. Once color development was achieved, the reaction was stopped, and the absorbance value was measured at 450 nm using the Infinite® 200 PRO microplate reader (TECAN, Switzerland). To quantify the serum IgG concentration against NoV VP1 protein, a standard curve was generated using a serial two-fold dilution of mouse IgG in 1×PBS.

Evaluation of T-Cell Responses by Flow Cytometer

Norovirus-specific T-cell responses were assessed in mouse splenocytes by intracellular cytokine staining (ICS) and flow cytometry. Initially, splenocytes were isolated from mouse spleens in RPMI medium using 100 µm cell strainers. After lysis the red blood cells and the splenocytes were incubated with NoV VP1 pooled peptides at the final concentration of 1 µg/mL. As positive controls, the cells were stimulated with PMA and Inomycin with a final concentration of 400 and 5 µg/mL, respectively. One hour later, the cells were blocked with brefeldin A (BFA), and the incubation continued for an additional 16 hours. Subsequently, the overnight-stimulated cells were harvested and stained with a fixable viability dye,

αCD4-PE and αCD8-Pacific Blue antibodies in FACs buffer (500 mL PBS + 5 mL FCS), before fixing and permeabilizing using the cytofix/cytoplasm solution (BD Bioscience). Intracellular cytokines were then stained using anti-INF-γ-FITC, anti-IL2-APC, and anti-TNFα-PeCy7 antibodies in 1× Perm/Wash buffer. After a 25-minute incubation on ice, the cells were washed with 1× Perm/Wash buffer and then with FACs buffer, before applying them to the FACs machine for analysis.[21]

Statistical Analysis

The statistical significance of the data was assessed by one-way ANOVA using GraphPad Prism 9.5.0. The threshold for statistical significance was set at $p < 0.05$. The results were presented as means ± standard deviation of the mean.

Results and Discussion

The synthesis of the Au-NPs was performed according to the Turkevich protocol, as illustrated in Figure 2. The Turkevich method is a well-established method that balances simplicity and control over particle characteristics. This method typically involves the reduction of gold ions in solution, often using trisodium citrate as both a reducing agent and a stabilizer. It is popular for its reproducibility and the relatively uniform size of the nanoparticles it produces. The observed color change from bright red in the first generation to progressively darker red in subsequent generations (2^{nd} to 4^{th}) was noteworthy.[22] The color of Au-NPs in solution results from their size and the inter-particle interactions, a phenomenon known as surface plasmon resonance (SPR).[23] A bright red color generally indicates smaller nanoparticles, while larger particles tend to exhibit a blue or purple color due to a shift in the SPR peak. The shift from bright to darker red could suggest a gradual increase in particle size and change in the distribution of sizes with each generation, possibly due to the stabilizing properties of the citrate ions or other environmental factors during synthesis. The stability of these nanoparticles is crucial for such applications, as unstable particles could aggregate or react in the cellular environment, leading to inconsistent results or potential cytotoxicity. For this reason, the 4^{th} generation of Au-NPs with the highest stability was used for the generation of PEI-conjugated Au-NPs and the evaluation of their potential for in vitro and in vivo gene delivery.

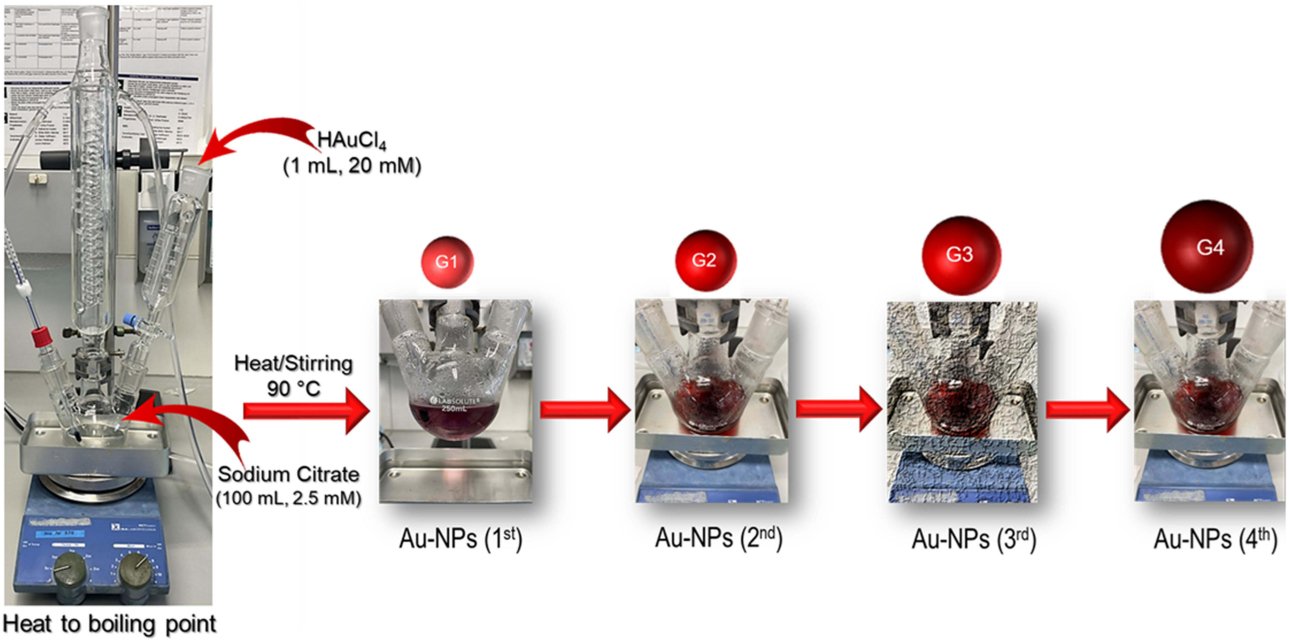

Figure 2 Diagrammatic representation of the synthesis process of Au-NPs by the Turkevich method.

https://doi.org/10.2147/IJN.S493211

Ultraviolet-Visible Spectroscopy Analysis (UV-Vis)

The presence of Au-NPs is confirmed by UV-vis spectra in Figure 3. The UV-vis spectrum provided a valuable tool for investigating the properties of Au-NPs. In this experiment, the UV-vis spectrum was utilized to monitor the growth of Au-NPs through gradual growth using citrate ions. The spectral analysis revealed a distinct red shift, indicating a progressive increase in the size of the NPs as the reaction progressed. At the inception of the reaction (1st), the UV-vis spectrum exhibited a peak wavelength of 524 nm with low absorbance.[24] This observation suggested the formation of primary nuclei of NPs, as the absorption of light by these nuclei was relatively weak. The color of the reaction also changed from yellow to bright red, which further confirmed the presence of Au-NPs. With the advancement of the growth process (2nd), the peak wavelength shifted slightly to 520 nm. However, the absorbance improved, indicating that the NPs became larger and more dispersed.[25] The spectral peak also sharpened, suggesting a higher degree of uniformity in the size distribution. In the 3rd generation, the peak wavelength further shifted to 527 nm, indicating a continued increase in the size of the NPs. However, the absorbance decreased compared to the 2nd generation.[25,26]

The observed shift in the peak wavelength from 524 to 530 nm in the UV-vis spectra of Au-NPs across generations indicates a redshift, consistent with an increase in nanoparticle size. Initially, this shift suggested increased agglomeration, reducing optical efficiency. However, as synthesis progressed to the 4th generation, the consistent peak at 530 nm and improved absorbance hinted at reduced aggregation and enhanced uniformity. The solution's deepening red hue further aligned with the size-dependent color changes in Au-NPs. These trends, in line with Mie theory, suggest that the larger Au-NPs exhibit a red shift due to more pronounced absorption at longer wavelengths.[27] This UV-vis spectral analysis effectively highlights the gradual growth of Au-NPs, validating the use of spectroscopy to monitor nanoparticle development and their size-related characteristics.

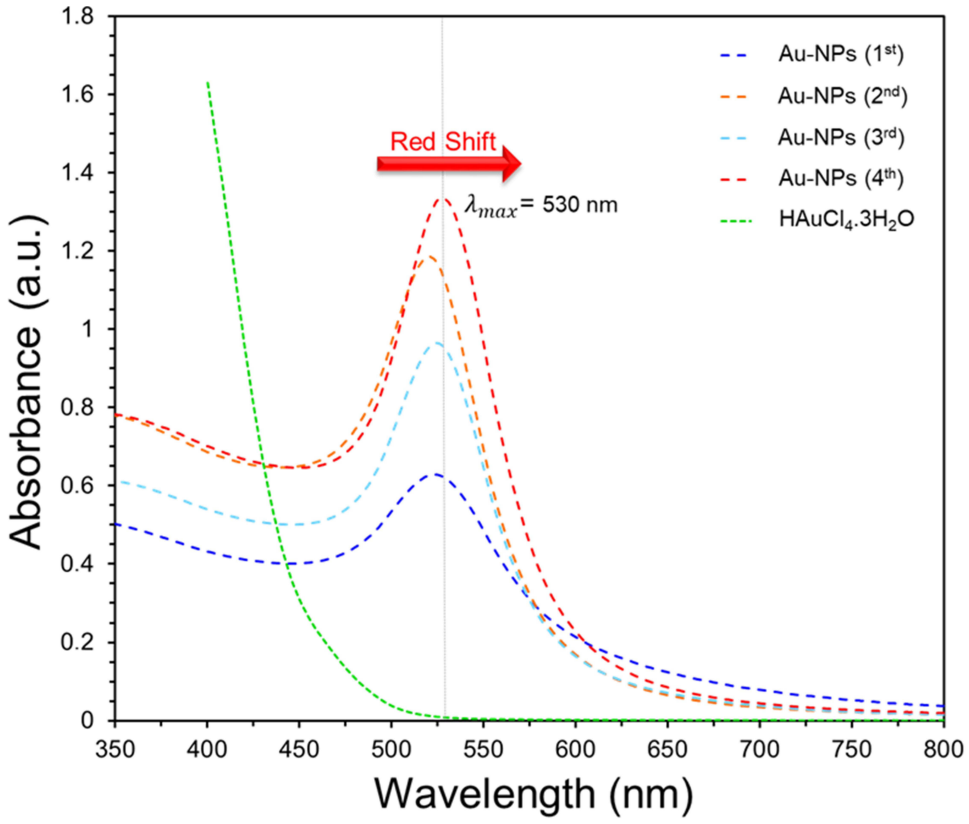

Figure 3 UV-vis spectra of Au-NPs prepared using the Turkevich method across various generations show a peak wavelength shift from 524 to 530 nm.

Transmission Electron Microscopy (TEM) Analysis

Transmission Electron Microscopy (TEM) was utilized to analyze the morphology and size of Au-NPs created through the Turkevich method, with an emphasis on their citrate-driven growth process. TEM imaging confirmed the spherical morphology of the Au-NPs, indicative of their successful synthesis. A steady increase in the average diameter of these nanoparticles was observed, from 14.06±1.56 nm in the first generation to 25.75±3.03 nm, 28.61±2.94 nm, and 31.52 ±3.45 nm in the second, third, and fourth generations, respectively (Figure 4).[28,29] This size escalation mirrored the expected growth trajectory over the generations. The measured sizes from TEM closely correlated with predictions from Mie's theory and particle size analysis, reinforcing the synthesis's efficacy. Notably, the second and fourth-generation Au-NPs showed minimal aggregation and possessed the most desirable morphology, suggesting these generations as optimal for achieving high-quality nanoparticles.[28] Consequently, Au-NPs from these generations were chosen for further studies, considering their uniformity, spherical shape, and optimal morphology. This TEM analysis sheds light on the controlled growth of Au-NPs in this synthesis approach.

Zeta Potential, and Average Size for Au-NPs

Measurement techniques for zeta potential (ζ-potential), such as electrophoretic mobility analysis and dynamic light scattering, are integral in characterizing NPs dispersions and assessing their colloidal stability. These measurements are critical for applications in drug delivery, imaging, and catalysis, where long-term stability of NP dispersions is essential for controlled release, precise targeting, and effective reaction rates. An investigation into the optimized ζ-potential and mean particle size of four generations of Au-NPs was conducted using the Turkevich synthesis protocol. The results, as detailed in Figure 5A, revealed that each generation of Au-NPs had a negative ζ-potential, which incrementally increased with each synthesis step. The average ζ-potentials for the first to fourth generations were −31.38, −27.96, −21.85, and −20.60 mV, respectively.[30] These figures suggest a relatively stable NP dispersion, with a slight decrease in stability due to increased particle loading.

Furthermore, the average size of the Au-NPs was observed to increase with each generation: 29.66 nm, 34.49 nm, 42.83 nm, and 52.09 nm, respectively (Figure 5B). This trend illustrates a significant correlation between the increasing size of NPs and the reduction in the absolute value of their surface charge in each successive generation.[31] Therefore, the observed trend of increasing particle size and decreasing ζ-potential across the generations in the synthesis of Au-NPs can be linked to the higher production rates associated with larger particles.

Zeta Potential Analysis of PEI-pDNA-Au-NPs

Due to its negatively charged, direct delivery of DNA plasmids into cells is challenging. To overcome this obstacle, DNA can be conjugated into nanocarriers and or cationic polymers, which possess a positive surface charge. This modification alters the overall charge of the DNA-nanocarrier complex, making it compatible with the negatively charged cell membrane and enabling efficient cellular uptake. Although Au-NPs offer promising properties for intracellular delivery, their negatively charged surface can hinder their efficient interaction with cells.[32] To address this challenge, a common approach involves conjugating Au-NPs to positively charged polymers, such as PEI, which can modify the overall charge of the NPs-DNA complex to a positive value (PEI-pDNA-Au-NPs). This positive charge enhances the electrostatic interaction between the conjugate and the negatively charged cell membrane, facilitating cellular uptake and intracellular delivery of the cargo. Additionally, positively charged PEI can further protect the encapsulated DNA from degradation by cellular nucleases, ensuring the delivery of intact and functional genetic material. By modifying the surface charge of Au-NPs with positively charged polymers, researchers can significantly improve their ability to deliver therapeutic molecules and gene editing tools into cells, paving the way for novel applications in drug delivery and gene therapy.[33] Figure 6a showed that the 4th-generation Au-NPs with a negative surface charge (−20.62 mV) were changed to a positive charge (+31.30 mV) when conjugated with a PEI.[34] Additionally, when plasmid DNA was linked with PEI and placed in the vicinity of Au-NPs (PEI-pDNA-Au-NPs), its surface charge became positive (+27.25 mV), but this value was less than the surface charge of PEI-Au-NPs, likely due to the interaction between the negatively charged plasmid DNA and the Au-NPs. This suggested that the surface charge of the PEI-Au-NPs complex was influenced by the presence of negatively charged plasmid DNA (Figure 6b).[35,36]

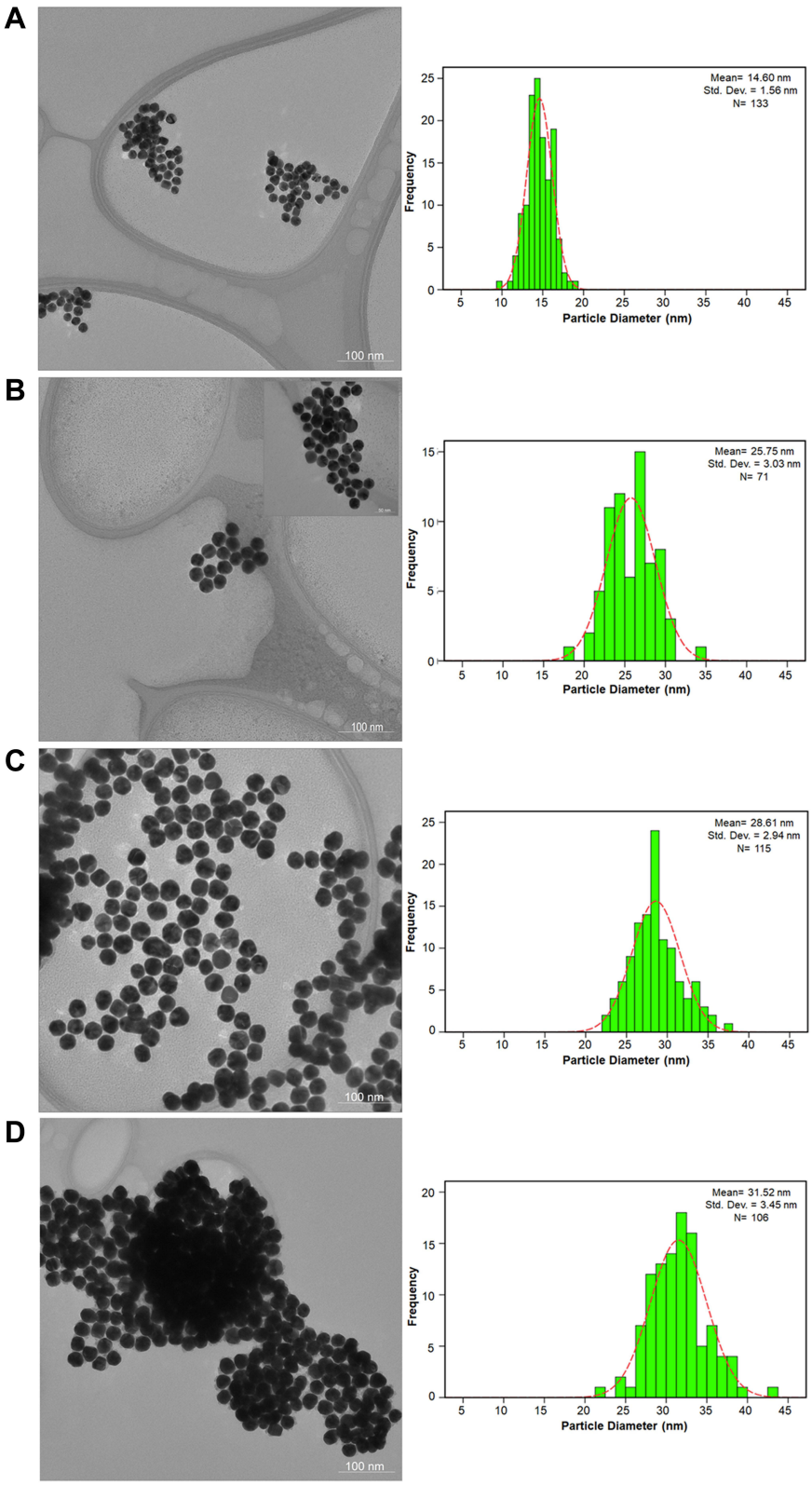

Figure 4 TEM images and their respective histograms illustrate the sequential stages of Au-NP synthesis via the Turkevich method. These representations capture the four progressive steps (**A–D**) in the nanoparticle growth process.

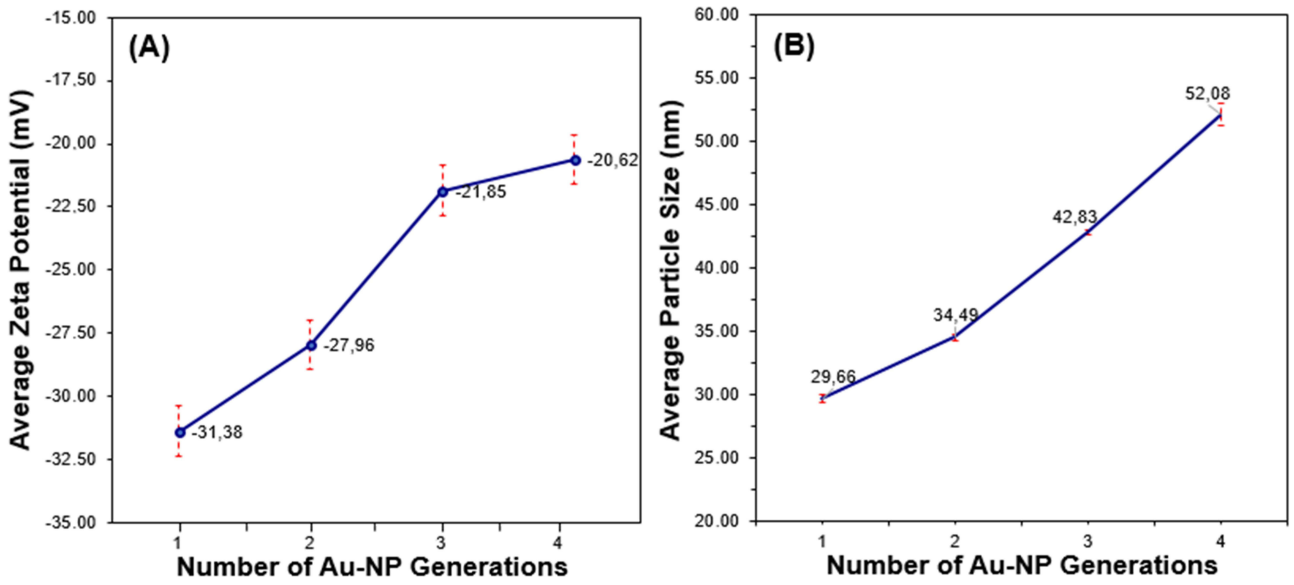

Figure 5 The images in parts (**A** and **B**) demonstrate a reduction in the absolute magnitude of the ζ potential concurrent with an increase in Au-NPs size across generations, correlated with alterations in colloidal stability.

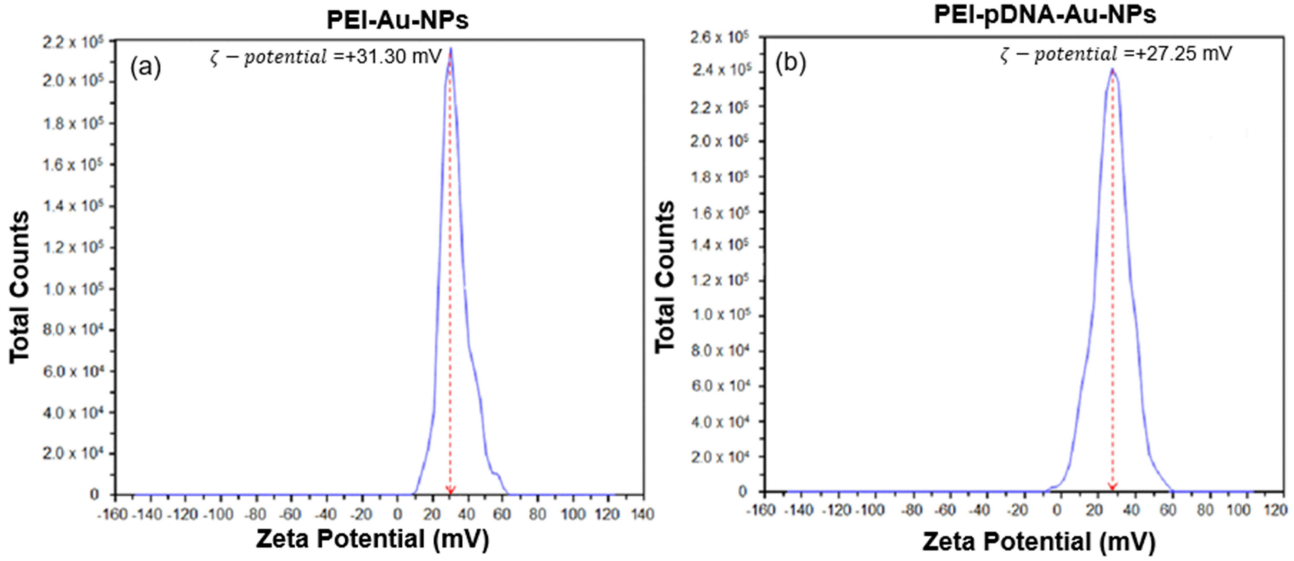

Figure 6 Zeta-potential values of 4th-generation Au-NPs linked with PEI (**a**). And PEI-Au-NPs conjugated with plasmid DNA (**b**). PEI conjugation significantly shifts the zeta potential towards positive values, indicating an increase in the surface charge of Au-NPs. This positively charged surface facilitates electrostatic interaction with the negatively charged cell membrane, promoting cellular uptake of the PEI-Au-NPs and PEI-pDNA-Au-NPs complex.

DNA Delivery in vitro Using Au-NPs

The primary aim of this study was to generate Au-NPs as an efficient DNA delivery system in eukaryotic cells. Here, we utilized a DNA plasmid encoding capsid protein of HuNoV GII.4 genotype, responsible for a significant number of acute gastroenteritis cases worldwide.[37] To assess this, both Au- and PEI-coated Au-NPs were assessed for their ability to deliver DNA plasmids into HEK293 cells.[38] The DNA plasmid pMN-NoVGII4 carries a GFP gene, allowing the screening of successful delivery of DNA plasmid by observing GFP expression under fluorescence microscopy, as depicted in Figure 7.[39] Significant protein expression was detected on day one post-transfection in the cells treated with DNA-loaded AuPEI-NPs, reaching 100% transfection efficacy by the second day. In contrast, in the cells treated with Au-NPs, a much lower proportion of green cells were detected, reaching approximately 30% of the cells two days post-

https://doi.org/10.2147/IJN.S493211

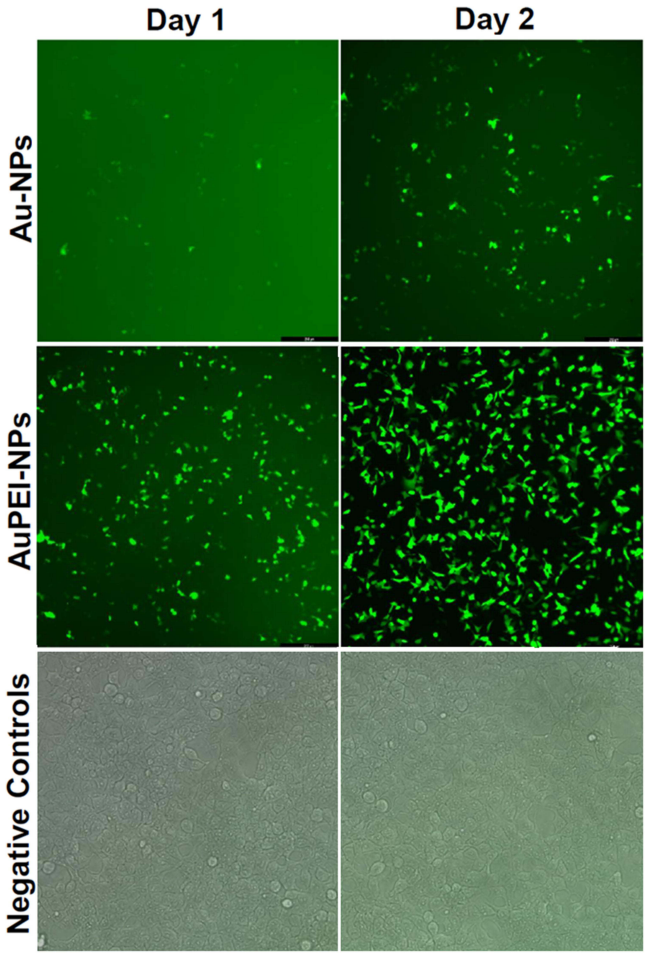

Figure 7 In vitro delivery of pDNA plasmids using Au-NPs and AuPEI-NPs. HEK293 cells were employed to assess the capability of Au-NPs for gene delivery in vitro. The cells were transfected with pDNA-loaded Au-NPs and AuPEI-NPs, and successful pDNA delivery was monitored over two days by observing green fluorescence protein under a fluorescence microscope.

transfection.[40] Notably, both nanoparticles showed no cytotoxic effects on the transfected cells during the experiment, indicating the safety aspect of the nanoparticles. These results highlight the potential of AuPEI-NPs for efficient delivery of DNA plasmids into eukaryotic cells.[41]

Efficient Delivery of DNA Plasmids Loaded on AuPEI-NPs in Mice

The main objective of this study was to evaluate the efficacy of Au-NPs as in vivo delivery vehicles for the DNA plasmid pMN-NoVGII4, intended as a potential DNA vaccine against the human NoV GII.4 genotype. To achieve this goal, both unmodified Au-NPs and PEI-conjugated Au-NPs were tested for their ability to deliver DNA plasmid in vivo and elicit immune responses against human NoV GII.4 in mice. The mice were injected with either DNA-loaded Au-NPs or DNA-loaded AuPEI-NPs (Figure 8a), with PBS or the DNA plasmid alone serving as controls. To assess the enhanced stimulation of specific immune responses following intramuscular administration of the DNA-loaded nanoparticles, serum samples were tested for NoV-specific IgG antibodies as the indicator for humoral immunity.[42] The results, summarized in Figure 8b, demonstrated a significant enhancement in DNA delivery and immunogenicity when Au-NPs were conjugated to PEI. Mice injected with DNA-loaded AuPEI-NPs exhibited a superior immune response compared to those injected with DNA-loaded Au-NPs alone. This was evidenced by the remarkably higher level of NoV-specific IgG antibodies in the serum samples ($p < 0.001$), indicating an enhanced humoral immune response (Figure 8b).

Furthermore, analysis of T-cell responses through intracellular cytokine staining (ICS) and flow cytometry revealed that PEI-coated Au-NPs also significantly improved the cellular responses. As shown in Figure 8c, in line with the results

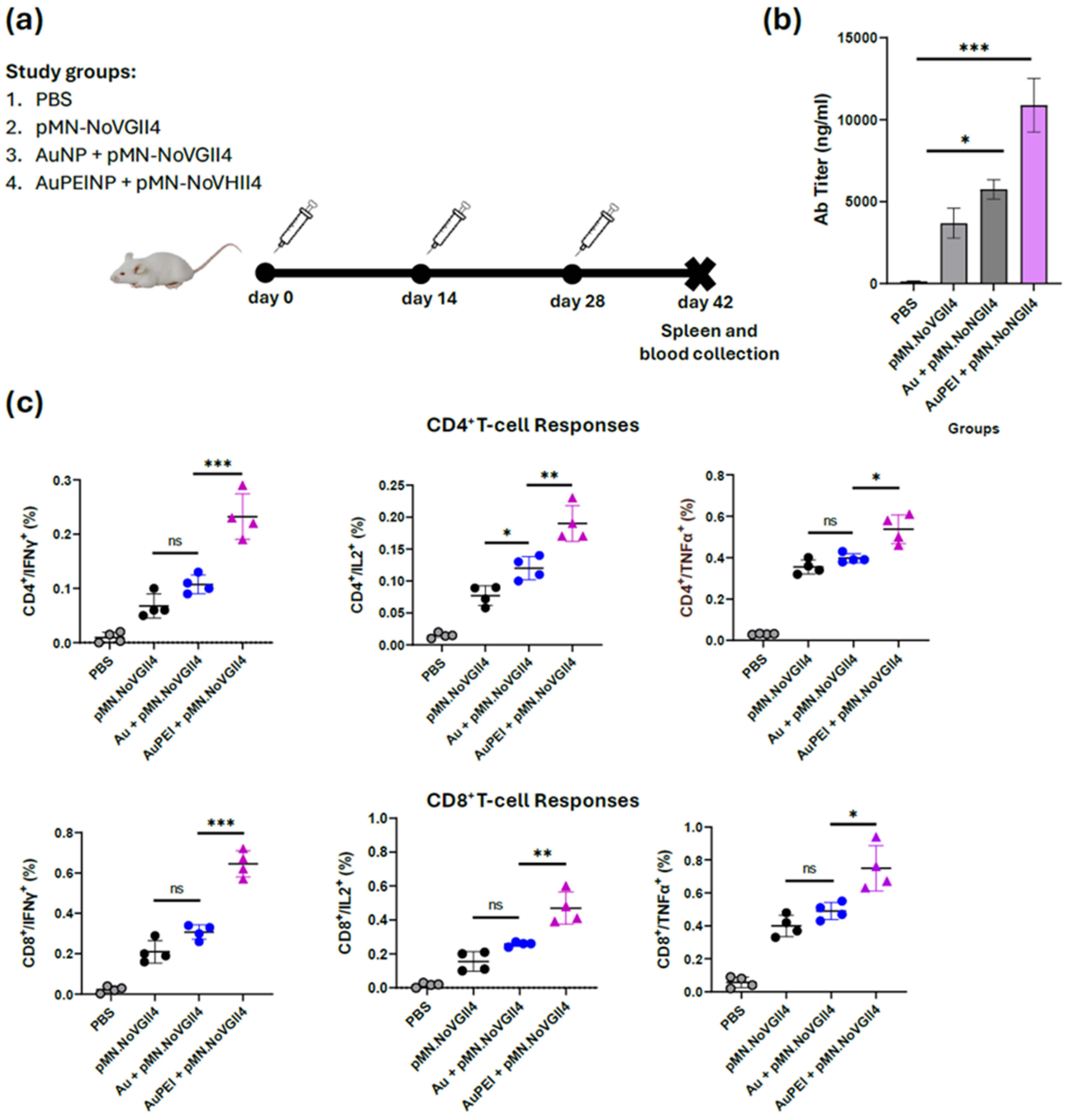

Figure 8 Evaluation of immune responses to pMN-NoVGII4 plasmid loaded on Au-NPs. BALB/c mice were tested for NoV-specific immune responses in intramuscular immunization using DNA-loaded Au-NPs, as compared to DNA plasmid alone. After the last administration (**a**), immune responses were assessed in mice by ELISA for antibody response (**b**) and intra-cellular staining in mice splenocytes for CD8+ and CD4+ T-cell responses (**c**). The star symbols indicate statistical significance, *p <0.05, **p <0.01, ***p <0.001.

for the antibody response, mice injected with DNA-loaded AuPEI-NPs exhibited higher frequencies of NoV-specific $CD8^+$ and $CD4^+$ T cells producing IFN-γ, IL,2 and TNF-α cytokines, compared to those injected with DNA-loaded Au-NPs alone. These cytokines are crucial markers of T cell-mediated immunity, which is essential for robust and protective immune response.[13]

The enhanced immune responses observed with PEI-conjugated Au-NPs can be attributed to the positive surface charge imparted by PEI, facilitating cell interaction and uptake of the nanoparticles.[43,44] This enhances the delivery of DNA plasmids into cells, thereby improving the expression of target antigen and subsequent immune responses. By

https://doi.org/10.2147/IJN.S493211

promoting endosomal escape, known as the "proton sponge effect", PEI also inhibits lysosomal degradation of the DNA-loaded NPs, increasing gene expression.[44,45] Consequently, PEI-coated NPs provide a reliable and controlled in vivo delivery system for DNA-based constructs.

PEI is also known to have adjuvant qualities, which can activate immune cells such as T and dendritic cells, which are crucial for both initiation and maintenance of immune responses to a target antigen.[13,36] Previous studies have shown that PEI, as adjuvant, boosting both innate and adaptive immune responses through activating interferon regulatory factor 3 (IRF3) pathway, resulting in the production of proinflammatory cytokines and type I interferons.[46] PEI-formulated vaccines also encourage B cells differentiation into plasma cells, maintaining sustained antibody production required for long-term protection against target pathogen.[47]

In contrast to PEI, lipid-based transfection reagents such as Lipofectamine have been shown to have high cytotoxicity and low biocompatibility, as their cationic lipid composition disrupts cell membranes, resulting in hepatotoxicity and inflammatory reactions when administered systemically.[48–51] This makes them inappropriate for gene delivery in vivo in human of animal models, although they are effective for in vitro DNA/RNA delivery. Other NP-based systems including dendrimers, polymeric nanoparticles, and viral vectors have been also investigated for gene delivery in vivo.[52–54] While viral-based vectors show high transfection efficiency, their safety issues limit their widespread application.[54] Dendrimers and polymeric NPs, similar to PEI-Au NPs, are nonviral delivery systems with adjustable characteristics, yet certain formulations show cytotoxic effects.[52,53] In contrast, by combining the stability tunability of gold NPs with the high binding capacity of PEI to DNA constructs, PEI-coated Au-NPs provide a distinct advantage over existing delivery systems, making it an effective vehicle for in vivo gene delivery.

Although our results proved the efficacy of PEI-coated Au-NPs in eliciting significant levels of immune responses in mice, additional studies into their possible accumulation in animal organs, and long-term effects and ideal formulation are recommended to guarantee their safety for use in clinical settings.

Conclusion

The present study successfully demonstrates the production and application of PEI-conjugated Au-NPs as an effective in vitro and in vivo gene delivery system. Utilizing the Turkevich method, Au-NPs were produced with regulated size and shape, which are critical for their stability and cellular uptake. The nanoparticles revealed a consistent rise in size over production, with the fourth generation showing the best features for DNA delivery. Coating with PEI significantly increased the transfection efficiency of Au-NPs in HEK293 cells. Furthermore, in vivo characterization demonstrated that DNA-loaded PEI Au-NPs elicited strong B-and T- immune responses in mice, indicating the potential of PEI-coated AU-NPs as a platform for DNA vaccine formulation.

These findings highlight the adaptability of PEI-coated Au-NPs for biomedical applications, particularly DNA-based vaccine formulation. The capability of the nanoparticles in enhancing transfection efficiency and immune stimulation in mice combined with their stability and tunability suggest the PEI-conjugated Au-NP as valuable tool for non-viral gene delivery, not only for DNA-based vaccine formulation but also for a wide range of therapeutic applications. Overall, this work provides valuable insights into the design of nanoparticle-based systems for DNA and gene delivery with potential application in DNA-based vaccination and gene therapy in clinical settings.

Ethics Statement

The study was conducted following protocols approved by the Department of Health, Consumer Protection, and Pharmacy, Government of Upper Bavaria (ROB-55.2-2532.Vet-02-18-77).

Acknowledgments

The authors would like to express their sincere gratitude to the Institute of Virology and the Catalysis Research Center at the Technical University of Munich for their invaluable support and resources. Special appreciation is extended to the laboratory staff for their assistance in the synthesis and characterization of Au-NPs, which played a crucial role in this research. Additionally, the authors acknowledge the financial support provided by the Deutsche Forschungsgemeinschaft (DFG) under project No. 528507260.

Disclosure

The authors report no conflicts of interest in this work.

References

1. Ferrando RM, Lay L, Polito L. Gold nanoparticle-based platforms for vaccine development. *Drug Discov Today Technol*. 2020;38:57–67. doi:10.1016/j.ddtec.2021.02.001
2. Shen Y, Hao T, Ou S, Hu C, Chen L. Applications and perspectives of nanomaterials in novel vaccine development. *MedChemComm*. 2018;9 (2):226–238. doi:10.1039/C7MD00158D
3. Compostella F, Pitirollo O, Silvestri A, Polito L. Glyco-gold nanoparticles: synthesis and applications. *Beilstein J Org Chem*. 2017;13:1008–1021. doi:10.3762/bjoc.13.100
4. Kohout C, Santi C, Polito L. Anisotropic gold nanoparticles in biomedical applications. *Int J mol Sci*. 2018;19(11):3385. doi:10.3390/ijms19113385
5. Zhang P, Chiu YC, Tostanoski LH, Jewell CM. Polyelectrolyte multilayers assembled entirely from immune signals on gold nanoparticle templates promote antigen-specific T-cell response. *ACS Nano*. 2015;9(6):6465–6477. doi:10.1021/acsnano.5b02153
6. Masomian M, Ahmad Z, Gew LT, Poh CL. Development of next-generation Streptococcus pneumoniae vaccines conferring broad protection. *Vaccines*. 2020;8:1–23.
7. Kus-Liśkiewicz M, Fickers P, Ben-Tahar I. Biocompatibility and cytotoxicity of gold nanoparticles: recent advances in methodologies and regulations. *Int J mol Sci*. 2021;22(20):10952. doi:10.3390/ijms222010952
8. Ho W, Gao M, Li F, Li Z, Zhang XQ, Xu X. Next-generation vaccines: nanoparticle-mediated DNA and mRNA delivery. *Adv Healthc Mater*. 2021;10(8):2001812. doi:10.1002/adhm.202001812
9. Santhosh PB, Genova J, Chamati H. Green synthesis of gold nanoparticles: an eco-friendly approach. *Chemistry*. 2022;4(2):345–369.
10. Lee KX, Shameli K, Yew YP, et al. Recent developments in the facile bio-synthesis of gold nanoparticles (AuNPs) and their biomedical applications. *Int J Nanomed*. 2020;15:275–300. doi:10.2147/IJN.S233789
11. Valatabar N, Oroojalian F, Kazemzadeh M, Mokhtarzadeh AA, Safaralizadeh R, Sahebkar A. Recent advances in gene delivery nanoplatforms based on spherical nucleic acids. *J Nanobiotechnology*. 2024;22(1):386. doi:10.1186/s12951-024-02648-5
12. Yeh YC, Creran B, Rotello VM. Gold nanoparticles: preparation, properties, and applications in bionanotechnology. *Nanoscale*. 2012;4 (6):1871–1880. doi:10.1039/C1NR11188D
13. Shen C, Jun L, Zhang Y, et al. Polyethylenimine-based micro/nano particles as vaccine adjuvants. *Int J Nanomed*. 2017;12:5443–5460. doi:10.2147/IJN.S137980
14. Xiang SD, Scholzen A, Minigo G, et al. Pathogen recognition and development of particulate vaccines: does size matter? *Methods*. 2006;40(1):1–9. doi:10.1016/j.ymeth.2006.05.016
15. Dobrovolskaia MA, McNeil SE. Immunological properties of engineered nanomaterials. *Nat Nanotechnol*. 2007;2(8):469–478. doi:10.1038/nnano.2007.223
16. Li Y, Tian H, Xiao C, Ding J, Chen X. Efficient recovery of precious metal based on Au–S bond and electrostatic interaction. *Green Chem*. 2014;16 (12):4875–4878.
17. Dong J, Carpinone PL, Pyrgiotakis G, Demokritou P, Moudgil BM. Synthesis of precision gold nanoparticles using Turkevich method. *Kona*. 2020;10(37):224–232. doi:10.14356/kona.2020011
18. Oliveira AEF, Pereira AC, Resende MAC, Ferreira LF. Gold nanoparticles: a didactic step-by-step of the synthesis using the Turkevich method, mechanisms, and characterizations. *Analytica*. 2023;4(2):250–263.
19. Tran M, DePenning R, Turner M, Padalkar S. Effect of citrate ratio and temperature on gold nanoparticle size and morphology. *Mater Res Express*. 2016;3:105027.
20. Afridi SQ, Moeini H, Kalali B, et al. Quantitation of norovirus-specific IgG before and after infection in immunocompromised patients. *Braz J Microbiol*. 2020;51(1):183–187. doi:10.1007/s42770-019-00176-1
21. Gioulbasani M, Tsagaratou A. Defining iNKT cell subsets and their function by flow cytometry. *Curr Protoc*. 2023;3(7):e838. doi:10.1002/cpz1.838
22. Jana J, Ganguly M, Pal T. Enlightening surface plasmon resonance effect of metal nanoparticles for practical spectroscopic application. *RSC Adv*. 2016;6(89):86174–86211. doi:10.1039/C6RA14173K
23. Sadrolhosseini AR, Noor ASM, Moksin MM. Application of surface plasmon resonance based on a metal nanoparticle. In: *Plasmonics Principles and Applications*. London, UK: IntechOpen; 2012:253–282.
24. Osonga FJ, Yazgan I, Kariuki V, et al. Greener synthesis and characterization, antimicrobial and cytotoxicity studies of gold nanoparticles of novel shapes and sizes. *RSC Adv*. 2016;6(3):2302. doi:10.1039/C5RA22906E
25. Noginov MA, Zhu G, Bohoura M, et al. The effect of gain and absorption on surface plasmons in metal nanoparticles. *Appl Phys B Lasers Opt*. 2007;86(3):455. doi:10.1007/s00340-006-2401-0
26. Henglein A. A physicochemical property of small metal particles in solution: "microelectrode" reactions, chemisorption, composite metal particles, and the atom-to-metal transition. *J Phys Chem*. 1993;97(21):457–5471. doi:10.1021/j100123a004
27. López-Muñoz GA, Pescador-Rojas JA, Ortega-Lopez J, Salazar JS, Balderas-López JA. Thermal diffusivity measurement of spherical gold nanofluids of different sizes/concentrations. *Nanoscale Res Lett*. 2012;7(1):423. doi:10.1186/1556-276X-7-423
28. Wrigglesworth EG, Johnston JH. Mie theory and the di chroic effect for spherical gold nanoparticles: an experimental approach. *Nanoscale Adv*. 2021;3(12):3530–3536. doi:10.1039/D1NA00148E
29. Volodymyr D, Olga K, Svitlana P, et al. Plasmonic colloidal Au nanoparticles in DMSO: facile synthesis and characterization. *RSC Adv*. 2022;12 (33):21591–21599. doi:10.1039/D2RA03605C
30. Malassis L, Dreyfus R, Murphy RJ, et al. One-step green synthesis of gold and silver nanoparticles with ascorbic acid and their versatile surface post-functionalization. *RSC Adv*. 2016;6(39):33092–33100. doi:10.1039/C6RA00194G
31. Behera M, Ram S. Inquiring the mechanism of formation, encapsulation, and stabilization of gold nanoparticles by poly (vinyl pyrrolidone) molecules in 1-butanol. *Appl Nanosci*. 2014;4(2):247–254. doi:10.1007/s13204-013-0198-9

32. Ghosh PS, Kim CK, Han G, Forbes NS, Rotello VM. Efficient gene delivery vectors by tuning the surface Charge density of amino acid-functionalized gold nanoparticles. *ACS Nano*. 2008;2(11):2213–2218. doi:10.1021/nn800507t
33. Gupta R, Rai B. Effect of size and surface charge of gold nanoparticles on their skin permeability: a molecular dynamics study. *Sci Rep*. 2017;7 (1):45292. doi:10.1038/srep45292
34. Zakeri A, Jadidi Kouhbanani MA, Beheshtkhoo N, et al. Polyethylenimine-based nanocarriers in co-delivery of drug and gene: a developing horizon. *Nano Rev Exp*. 2018;9(1):1488497. doi:10.1080/20022727.2018.1488497
35. Bali K, Bak M, Szarka K, et al. Controlling the morphology of poly(ethyleneimine)/gold nano-assemblies through the variation of pH and electrolyte additives. *J mol Liq*. 2021;322(114559):1–11. doi:10.1016/j.molliq.2020.114559
36. Srijampa S, Buddhisa S, Ngernpimai S, et al. Influence of gold nanoparticles with different surface charges on localization and monocyte behavior. *Bioconjugate Chem*. 2020;31(4):1133–1143.
37. Turner MD, Nedjai B, Hurst T, Pennington DJ. Cytokines and chemokines: at the crossroads of cell signaling and inflammatory disease. *Biochim. Biophys. Acta*. 2014;1843(11):2563–2582. doi:10.1016/j.bbamcr.2014.05.014
38. Gu Y, Lian Y, Zheng Q, et al. Association among cytokine profiles of innate and adaptive immune responses and clinical-virological features in untreated patients with chronic hepatitis B. *BMC Infect Dis*. 2020;20(1):509. doi:10.1186/s12879-020-05233-x
39. Christina G, Jean-Christophe L, Michael B. The intracellular visualization of exogenous DNA in fluorescence microscopy. *Drug Delivery Trans Res*. 2024;14(8):2242. doi:10.1007/s13346-024-01563-4
40. Von Arnim AG, Deng XW, Stacey MG. Cloning vectors for the expression of green fluorescent protein fusion proteins in transgenic plants. *Gene*. 1998;221(1):35. doi:10.1016/s0378-1119(98)00433-8
41. Petersen S, Soller JT, Wagner S, et al. Co-transfection of plasmid DNA and laser-generated gold nanoparticles does not disturb the bioactivity of the GFP-HMGB1 fusion protein. *J Nanobiotechnology*. 2009;7(1):1–6. doi:10.1186/1477-3155-7-6
42. Mulens-Arias V, Nicolás-Boluda A, Carn F, Gazeau F. Cationic polyethyleneimine (PEI)-gold nanocomposites modulate macrophage activation and reprogram mouse breast triple-negative MET-1 Tumor immunological microenvironment. *Pharmaceutics*. 2022;14(10):2234. doi:10.3390/pharmaceutics14102234
43. Thomas M, Klibanov AM. Conjugation to gold nanoparticles enhances polyethylenimine's transfer of plasmid DNA into mammalian cells. *Proc Natl Acad Sci USA*. 2003;100(16):9138–9143. doi:10.1073/pnas.1233634100
44. Boussif O, Lezoualc'h F, Zanta MA, et al. A versatile vector for gene and oligonucleotide transfer into cells in culture and in vivo: polyethylenimine. *Proc Natl Acad Sci USA*. 1995;92(16):7297–7301. doi: 10.1073/pnas.92.16.7297.
45. Akinc A, Thomas M, Klibanov AM, Langer R. Exploring polyethylenimine-mediated DNA transfection and the proton sponge hypothesis. *J Gene Med*. 2005;7(5):657–663. doi:10.1002/jgm.696
46. Sheppard NC, Brinckmann SA, Gartlan KH, et al. Polyethyleneimine is a potent systemic adjuvant for glycoprotein antigens. *Int Immunol*. 2014;26 (10):531–538. doi:10.1093/intimm/dxu055
47. Jin Z, Dong YT, Liu S, et al. Potential of polyethyleneimine as an adjuvant to prepare long-term and potent antifungal nanovaccine. *Front Immunol*. 2022;16(13):843684. doi:10.3389/fimmu.2022.843684
48. Lv H, Zhang S, Wang B, Cui S, Yan J. Toxicity of cationic lipids and cationic polymers in gene delivery. *J Control Release*. 2006;114(1):100–109. doi:10.1016/j.jconrel.2006.04.014
49. Khalil IA, Kogure K, Akita H, Harashima H. Uptake pathways and subsequent intracellular trafficking in nonviral gene delivery. *Pharmacol Rev*. 2006;58(1):32–45. doi:10.1124/pr.58.1.8
50. Zhang S, Xu Y, Wang B, Qiao W, Liu D, Li Z. Cationic compounds used in lipoplexes and polyplexes for gene delivery. *J Control Release*. 2014;100(2):165–180.
51. Wang T, Larcher LM, Ma L, Veedu RN. Systematic screening of commonly used commercial transfection reagents towards efficient transfection of single-stranded oligonucleotides. *Molecules*. 2018;23(10):2564. doi:10.3390/molecules23102564
52. Dufès C, Uchegbu IF, Schätzlein AG. Dendrimers in gene delivery. *Adv. Drug Delivery Rev*. 2005;57(15):2177–2202. doi:10.1016/j.addr.2005.09.017
53. Zhang L, Gu F, Chan J, Wang A, Langer R, Farokhzad O. Nanoparticles in medicine: therapeutic applications and developments. *Clin. Pharmacol. Ther*. 2008;83(5):761–769. doi:10.1038/sj.clpt.6100400
54. Lukashev AN, Zamyatnin AA. Viral vectors for gene therapy: current state and clinical perspectives. *Biochemistry*. 2016;81(7):700–708. doi:10.1134/S0006297916070063